DUNNE Project: Preprint

Victor Hoffmann[1], Ilias Nahmed[1], Guenael Cabanes[2], Parisa Rastin[2], Julien Boisse[3]

1: École Nationale Supérieure des Mines de Nancy

2: Lorraine Research Laboratory in Computer Science and its Applications (LORIA)

3: Laboratory of Energies, Theoretical and Applied Mechanics (LEMTA)

August 28, 2023

Contents

1 Introduction

In the context of the climate crisis and resource scarcity, industries are increasingly turning towards recyclable and environmentally friendly materials.

Composite materials are now pivotal in many sectors (energy, transportation, etc.) due to their lightweight nature, stress and corrosion resistance, as well as thermal insulation properties. The mechanical properties of composite materials are heavily dependent on their microstructure, including the size, shape, distribution, and orientation of their constituent materials. With the aim of maximizing product and system performance while minimizing the carbon footprint across their lifecycle, it becomes essential to comprehend how microstructures influence the performance of composite materials. This understanding could lead to the creation of composites with specific properties.

The **DUNNE project** (***D****esign and mechanical analysis of composites microstr****U****ctures with artificial* ***N****eural* ***NE****tworks*) seeks to contribute to the design of these composite materials by establishing a link between their microstructure and mechanical properties. This approach enables us to determine the mechanical behavior of composite materials based on their microstructure and vice versa. To achieve this, we intend to employ machine learning methods, particularly neural networks.

In this article, our focus is solely on predicting the Dynamic Mechanical Analysis (DMA) curves of unidirectional fiber composites as a function of frequency.

2 RVE's and DMA

2.1 Representative Volume Element (RVE)

Representative Volume Elements (RVEs) are a key concept for accurately modeling material properties. An RVE is a small portion of material that can alone capture the overall appearance and composition of the material. This volume is chosen in such a way that the microscopic properties of the material inside the RVE are statistically similar to those of the material as a whole. In a sense, it's a generalization of the "unit cell" of a crystal lattice.

RVEs are highly useful as they allow us to reduce the dimension of material analysis. By focusing on the representative volume element, we can significantly cut down on costs and computation time without losing generality.

Determining the RVE of a material is a problem in itself, but for our study, we will be working with materials simulated on the machine. Hence, the RVE is, in a way, defined through construction. What's important to note is that our microstructures will be modeled by 3D images (possibly 2D if studying a cross-section of an RVE), forming the foundation of our dataset for the predictive model of material physical characteristics.

2.2 Dynamic Mechanical Analysis (DMA)

Dynamic Mechanical Analysis (DMA) is an experimental technique used to characterize the mechanical properties of materials. It allows for the study of a material's behavior under dynamic mechanical stresses, such as oscillatory deformation, frequency, and temperature.

DMA measures the viscoelastic properties of materials, meaning it examines both the elastic response (recovery after deformation) and the viscous response (energy dissipation during deformation). This provides insights into how a material reacts and behaves under various mechanical constraints.

The fundamental principle of DMA involves applying oscillatory mechanical stress to a material sample while measuring its mechanical responses, such as deformation, stress, and temperature, over time. The collected data is then utilized to determine the material's mechanical properties, including the storage modulus (elasticity) and loss modulus (viscosity), as well as other parameters related to viscoelasticity. These properties are typically represented by a complex modulus.

Using oscillatory machines, one can vary either the oscillation frequency at a fixed temperature or the temperature at a fixed frequency. This allows for the representation of the elastic modulus (real part of the signal) and the loss modulus, which is proportional to the energy irreversibly transformed into heat (imaginary part of the signal), as functions of temperature or frequency. **Hence, it is these DMA curves that will represent the mechanical properties of composite materials**, which we aim to determine based on microstructure images. A DMA example based on microstructure can be found in section 5.

3 State of the Art

Obtaining physical properties of simulated composite materials is a complex challenge that requires many calculations and considerable computation time when using classical methods like finite elements (FEM). With the advent of deep learning methods, a new approach to solving these issues has arisen, especially Convolutional Neural Networks (CNNs). During the last few years, CNNs have proven to be quite efficient when dealing with these problems. In 2018, Zijiang Yang & al. [5] implemented 3D CNNs for the first time to model elastic homogenization linkages of 3D images of composite materials. In 2020, Yixing Wang & al. [3] used this approach for a similar problem: predicting the mean value of the glassy and rubbery moduli given the 3D images of microstructures. Many other papers were published in this wake; nevertheless, none aimed to predict the whole curve of glassy and rubbery moduli to our knowledge. Hence, there is not a true benchmark available to compare our model to, apart from traditional methods of physics simulations. In many papers published, other techniques have been implemented to improve or simplify the CNN models used. For instance, A. Mann and S. Kalidindi [1] worked on combining CNNs with correlation maps of microstructures implemented via the two-point statistics method, which proved to be an approach that takes little time to train and provides acceptable results. This motivates us to try such techniques to develop a robust and accurate model.

4 Experimentation

4.1 Dataset

The input data consists of 15 000 distinct configurations of representative volume elements (RVEs) for unidirectional fiber-reinforced composite materials. All RVEs adhere to periodic boundary conditions. The fibers all have the same radius and vary from 1 to 150 per RVE, with volume fractions ranging from 0.05 (5%) to 0.75 (75%). A total of 100 random configurations have been simulated for each volume fraction (with a step of 0.005)

Typically, RVEs are represented in three-dimensional matrices, but since we are studying unidirectional fiber materials, a cross-section of each matrix is sufficient. As a result, they will be represented by two-dimensional matrices of size 256×256, where each element is either 0.5 (filler) or -0.5 (matrix). An example of a RVE representation is given in figure 1.

The output data consists of a set of two dynamic mechanical analysis (DMA) curves for each RVE: the shear storage modulus and the shear loss modulus, both provided in MPa as a function of the given angular frequency in $\mathrm{rad\,s^{-1}}$. Each curve is represented by a collection of 30 data points provided on a logarithmic scale of angular frequency. The objective of our model is thus to predict these two curves solely based on the representations of the RVEs. It turns out that under shear stress, both the shear storage modulus and the shear loss modulus remain invariant under a 90° rotation and horizontal and vertical symmetries of the RVE.

In order for the model to understand periodic boundary conditions, the data has been augmented with 4 random (2 horizontal and 2 vertical) translations of each RVE. The computer's used RAM (32 GB) did not allow for further data expansion. Regarding the invariance under 90° rotation, horizontal, and vertical symmetry, we opted for an equivariant convolutional neural network [4] instead of data augmentation (cf. 4.2). 70% of the data was used for training the model, 15% was used for model validation, and the remaining 15% was used for model testing. The batch size chosen for our model is 40.

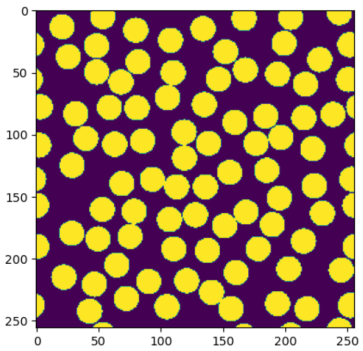

Figure 1: Example of the representation of a Representative Volume Element (RVE). The RVE is depicted as a 256×256 matrix, where each element takes on a value of either 0.5 (filler) or -0.5 (matrix). All RVEs adhere to periodic boundary conditions.

4.2 Equivariant Convolutional Neural Networks

Convolutional Neural Networks (CNNs) have gained substantial attention in recent years due to their effective performance in image processing tasks. However, traditional CNNs are not equipped to deal with transformations or symmetries in the input data. This limitation prompted the development of Equivariant Steerable CNNs (ESCNNs) [4], a form of convolutional neural network designed to handle specific transformations, such as rotations and symmetries without the need to see all possible transformed versions of the input data during training.

Let's denote the input to a layer as x, the transformed version of this input as $T(x)$ where T is the transformation (for instance, rotation), and let f denote the layer's operation. Then, the layer is equivariant if there exists a transformation T' such that for all inputs x:

$$f(T(x)) = T'(f(x)) \tag{1}$$

(1) means that applying the transformation to the input and then applying the layer operation is the same as applying the layer operation first and then transforming the output. Such equivariances are achieved through the use of steerable filters.

Steerable filters are special kinds of filters whose responses can be computed for any rotated version from a limited set of basis filters. This property gives them the power to detect features irrespective of their orientation in the image, making the network more robust and efficient. Specifically, in the context of ESCNNs, the steerability of these filters helps in achieving rotational equivariance.

Therefore, ESCNNs have allowed us to make our model remain invariant under a 90° rotation and horizontal and vertical symmetries of the RVE without data augmentation. However, this has a computational cost since for each equivariant convolutional block, we have 8 parallel convolutional blocks (1 for each unique combination of 90° rotation and symmetry).

4.3 Architecture of the model

The figure 2 shows a scheme of the architecture's model.

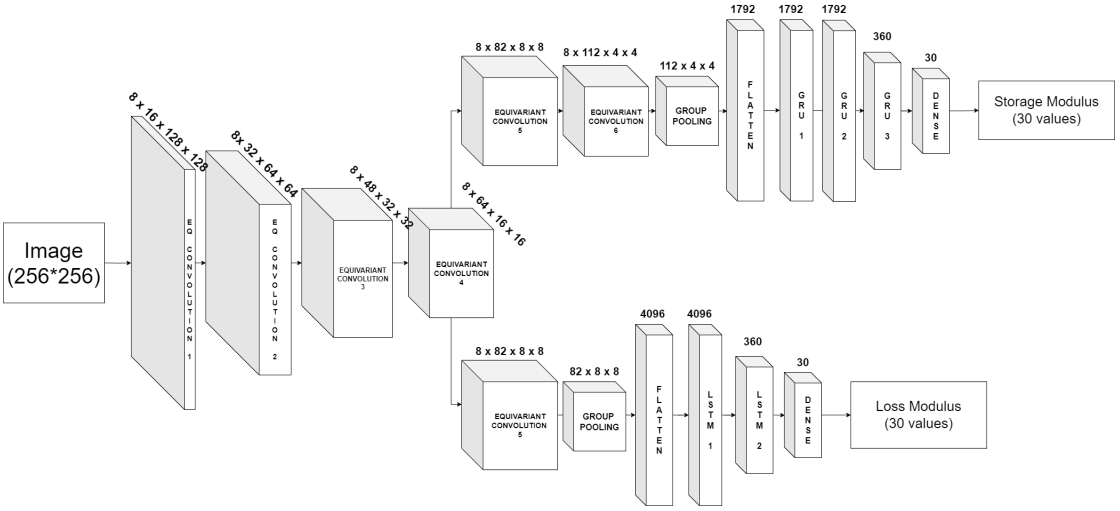

Figure 2: Architecture of the multi-task model. It consists of a common equivariant convolutional component, which divides itself into two branches: one for the shear storage modulus and another for the shear loss modulus.

As our objective is to concurrently predict both the shear storage modulus and the shear loss modulus, we have opted for a multi-task model. This model consists of a common equivariant convolutional component, which subsequently diverges into two branches: one for the shear storage modulus and another for the shear loss modulus. Each branch is composed of at least one equivariant convolutional block, and several layers of Recurrent Neural Networks (RNNs).

Each convolutional block is composed of an equivariant convolutional layer with a kernel size of 3×3 and circular padding, a batch normalization layer to which we apply the ReLU activation function and an Antialiased MaxPooling layer. The purpose of the Antialiased MaxPooling is to apply MaxPooling to the kernel which has undergone a Gaussian filter that slightly blurs the kernel [6]. This enables the ESCNN to be invariant to slight translations of the image, allowing it, in conjunction with circular padding, to better comprehend the notions of periodic boundary conditions.

At the end of the convolutional blocks in both branches, a group pooling is applied. Group pooling aggregates the eight different convolutional blocks executed in parallel for each rotation/symmetry combination in order to extract features invariant to such transformations [4].

The two branches are not identical. The branch for the shear storage modulus comprises two equivariant convolutional blocks and three layers of Gated Recurrent Units (GRUs), between which we have applied a Dropout rate of 0.2. It turns out that the shear storage modulus is more sensitive to short-term dependencies and requires more feature extraction than the shear loss modulus. Conversely, the branch for the shear loss modulus has only one equivariant convolutional block and two layers of Long Short-Term Memory (LSTM) units, between which we have implemented a Dropout rate of 0.3. At the end of each RNN block in both branches, a Fully Connected layer is applied to obtain values in $\mathbb{R}$. Indeed, in Pytorch, the output of RNNs falls between 0 and 1, due to a sigmoid activation function that is implicitly applied [2].

4.4 Performance metric

The scale of both the shear storage modulus and the shear loss modulus varies according to the volume fraction of the microstructures given as input. The lower the volume fraction, the lower the minimum and maximum of each modulus. To avoid the model giving too much importance to error minimization on moduli of microstructures with high volume fractions and not enough importance to low volume fractions, a relative loss function is necessary. The Mean Absolute Percentage Error (MAPE) is a classic choice for these types of situations. However, it poses problems for several loss modulus values that are very close to 0 for some low volume fraction cases, thus causing an explosion of this latter. To address this issue, we have opted for the weighted Mean Absolute Percentage Error (wMAPE) which is defined for each batch and each modulus as:

$$\text{wMAPE} = \frac{1}{N_{\text{seq.}}} \sum_{j \in \text{seq.}} \sum_{i \in \text{batch}} \frac{|y_{ij} - \hat{y}_{ij}|}{|y_{ij}|} \tag{2}$$

where seq. stands for sequence, which is the discrete representation of the storage or loss modulus, $N_{\text{seq}} = 30$, y_{ij} is the j^{th} point of the i^{th} sequence in the batch and $\hat{y_{ij}}$ is the prediction of y_{ij}. As shown in (2) for each point of the moduli, we calculate the average absolute difference between the real and the predicted value of the batch, then we divide it by the average real value of the batch. Finally, we take the average batch error of each point of each modulus and sum the two error modulus. Therefore, the performance metric is equal to $\text{wMAPE}_{\text{storage}} + \text{wMAPE}_{\text{loss}}$. In the section 5, the Mean Absolute Error (MAE) will also be provided for reference, which is defined for each batch and each modulus as:

$$\text{MAE} = \frac{1}{N_{\text{seq.}}} \sum_{j \in \text{seq.}} \frac{1}{N_{\text{batch}}} \sum_{i \in \text{batch}} |y_{ij} - \hat{y_{ij}}| \tag{3}$$

with the same notations as in (2) and $N_{\text{batch}} = 40$.

Regarding the optimizer, we have chosen Adam, with a learning rate of 0.001 and an L^2 regularization term with α set to 0.0001.

5 Results

The table 1 shows the MAE and wMAPE of the model for both shear storage modulus and shear loss modulus. Each mean error also includes its standard deviation. As mentioned in 3, to the best of our knowledge, no prior literature exists that endeavors to predict the complete set of Dynamic Mechanical Analysis (DMA) curves for both shear storage modulus and shear loss modulus as functions of frequency. Consequently, we lack a benchmark against which to compare our findings. As depicted in Figure 3, the challenge in predicting the loss modulus primarily lies within the range of intermediate frequencies, with values at the extremes being nearly negligible. Regarding the storage modulus, the difficulty of prediction often arises for high-frequency values.

With the purpose of assessing the robustness of our model, we conducted an analysis of its performance on each RVE as a function of the volume fraction. As depicted in Figure 4, the model demonstrates robustness in predicting storage moduli for RVEs which volume fraction ranges from 0.07 to 0.73. However, the model's robustness appears to diminish when predicting loss moduli for RVEs with volume fractions near 0.3 or 0.5. Additionally, the uncertainty of the loss modulus is higher than the uncertainty of the storage modulus. The MAPE of the loss modulus for volume fractions between 0.05 and 0.1 is challenging to interpret, because the loss modulus exhibits values very close to 0, which leads to a divergence in the MAPE values.

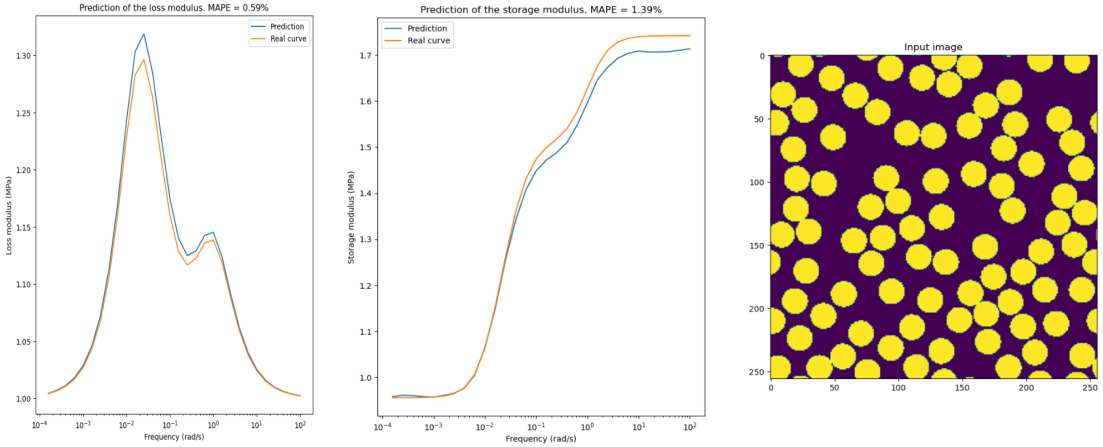

Figure 3: Prediction example of shear storage and loss moduli. Please take note that this concerns the Mean Absolute Percentage Error (MAPE), not the previously used weighted MAPE (wMAPE). Indeed, when there is just one prediction curve compared to a real curve (which is equivalent to a batch size set to 1), the wMAPE is equivalent to the MAPE.

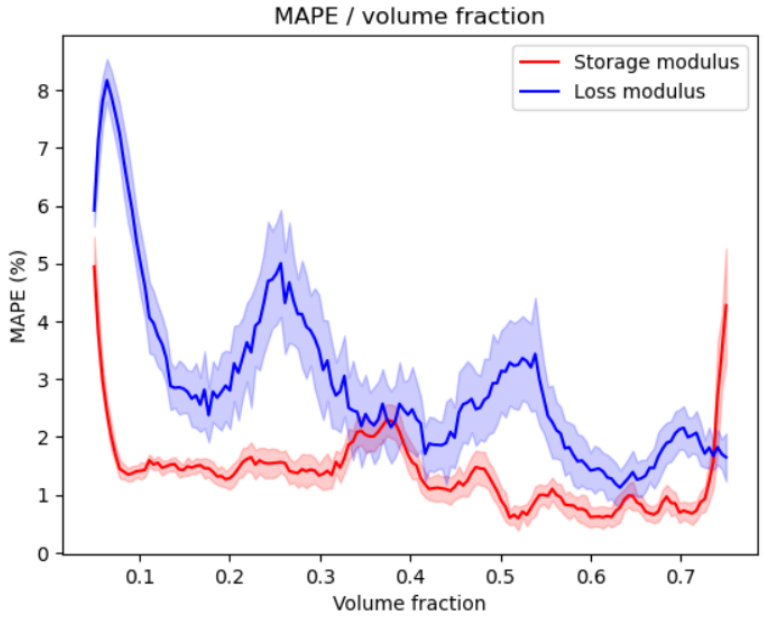

Figure 4: MAPE as a function of volume fraction. The average value of MAPE for each volume fraction has been plotted as a solid line, and the standard deviation of this value is depicted by the interval around the mean value. As mentioned in figure 3, please take note that this concerns the Mean Absolute Percentage Error (MAPE), not the previously used weighted MAPE (wMAPE). To generate such curves, the model was assessed on each RVE separately, employing a batch size of 1, as opposed to the previous procedure.

Table 1: wMAPE and MAE metrics of the model evaluated on the test set. The model has been trained on the wMAPE, the MAE is provided for reference.

	Shear Storage Modulus	Shear Loss Modulus
wMAPE	0.83% +/- 0.13%	1.85% +/- 0.25%
MAE	0.0134 +/- 0.0027	0.0025 +/- 0.0005

References

[1] Andrew Mann and Surya R. Kalidindi. Development of a Robust CNN Model for Capturing Microstructure-Property Linkages and Building Property Closures Supporting Material Design. *Frontiers in Materials*, 9:851085, March 2022. URL: https://www.frontiersin.org/articles/10.3389/fmats.2022.851085/full, doi:10.3389/fmats.2022.851085.

[2] Adam Paszke, Sam Gross, Francisco Massa, Adam Lerer, James Bradbury, Gregory Chanan, Trevor Killeen, Zeming Lin, Natalia Gimelshein, Luca Antiga, Alban Desmaison, Andreas Köpf, Edward Z. Yang, Zach DeVito, Martin Raison, Alykhan Tejani, Sasank Chilamkurthy, Benoit Steiner, Lu Fang, Junjie Bai, and Soumith Chintala. Pytorch: An imperative style, high-performance deep learning library. *CoRR*, abs/1912.01703, 2019. URL: http://arxiv.org/abs/1912.01703, arXiv:1912.01703.

[3] Yixing Wang, Min Zhang, Anqi Lin, Akshay Iyer, Aditya Shanker Prasad, Xiaolin Li, Yichi Zhang, Linda S. Schadler, Wei Chen, and L. Catherine Brinson. Mining structure–property relationships in polymer nanocomposites using data driven finite element analysis and multi-task convolutional neural networks. *Mol. Syst. Des. Eng.*, 5:962–975, 2020. URL: http://dx.doi.org/10.1039/D0ME00020E, doi:10.1039/D0ME00020E.

[4] Maurice Weiler and Gabriele Cesa. General E(2)-Equivariant Steerable CNNs. In *Conference on Neural Information Processing Systems (NeurIPS)*, 2019.

[5] Zijiang Yang, Yuksel C. Yabansu, Reda Al-Bahrani, Wei-keng Liao, Alok N. Choudhary, Surya R. Kalidindi, and Ankit Agrawal. Deep learning approaches for mining structure-property linkages in high contrast composites from simulation datasets. *Computational Materials Science*, 151:278–287, August 2018. URL: https://linkinghub.elsevier.com/retrieve/pii/S0927025618303215, doi:10.1016/j.commatsci.2018.05.014.

[6] Richard Zhang. Making convolutional networks shift-invariant again. *CoRR*, abs/1904.11486, 2019. URL: http://arxiv.org/abs/1904.11486, arXiv:1904.11486.